ANALYSIS OF ADDITIVELY CONTAMINATED LORENTZIANS BY INTEGRATION

BERND LINDEMANN
Second Department of Physiology, University of the Saarland, D-6650 Homburg/Saar, Federal Republic of Germany

ABSTRACT The two Lorentzian parameters, plateau power and corner frequency, can be retrieved from scattered spectral data points by forming the ratio of two numerical integrals of the data. With a small modification of this strategy, Lorentzians may be stripped from additive background spectra of unknown spectral shape. Recursive curve fitting is not required.

The current fluctuations generated by ion-transporting channels, which switch spontaneously between an open and closed state, often obey simple kinetics that result in single Lorentzians in the power spectrum of the process. The Lorentzian function is

$$G(f) = G_O / [1 + (f/f_c)^2], \qquad (1)$$

where f is frequency and G_O and f_c stand for plateau power and corner frequency, respectively. Mainly because of the limited amount of data entering the analysis, the spectral data points usually scatter, even in averaged spectra. Therefore, recursive numerical fitting with Eq. 1 is often used to retrieve G_O and f_c. The limited bandwidth of the records typically results in power spectra where only a few scattered data points are found at the Lorentzian plateau. This becomes particularly evident when the data are condensed (by smoothing over frequencies; e.g., Bendat and Piersol, 1971, p. 191. Conti et al., 1976) and displayed in double logarithmic coordinates (Fig. 1 *A*). Consequently the uncertainty of the values found for G_O and f_c is often large, as discussed earlier by Anderson and Stevens (1973).

To solve for the two unknowns, G_O and f_c, of Eq. 1, only two observations are needed, which should be as free of scatter as possible. Because random scatter is eliminated by integration,[1] it is practical to convert the many spectral data points into two integrals[2] and to calculate G_O and f_c from them. This is an alternative to nonlinear least-squares regression analysis.

Suppose the spectrum extends from f_0 to f_4 and includes the frequencies f_1, f_2, and f_3 such that the interval f_1 to f_2 contains f_c while f_2 to f_3 delimits a section of the Lorentzian tail as shown in Fig. 1 *A*. By integrating the Lorentzian data numerically from f_1 to f_3 and from f_2 to f_3, one obtains the two bandwidth-limited variances V_{13} and V_{23}. By integrating Eq. 1 within these limits, we find

$$V_{13} = G_O \cdot f_c \cdot (\arctan f_3/f_c - \arctan f_1/f_c), \qquad (2)$$

$$V_{23} = G_O \cdot f_c \cdot (\arctan f_3/f_c - \arctan f_2/f_c). \qquad (3)$$

Therefore, f_c is uniquely determined by the variance ratio:

$$\beta = \frac{V_{13}}{V_{23}} = \frac{\arctan f_3/f_c - \arctan f_1/f_c}{\arctan f_3/f_c - \arctan f_2/f_c} > 1, \qquad (4)$$

from which f_c is obtained by iterative approximations, using, for instance, a bisection protocol. Then G_O is calculated as follows:

$$G_O = \frac{V_{13}}{f_c \cdot (\arctan f_3/f_c - \arctan f_1/f_c)}. \qquad (2a)$$

Typically, the Lorentzian spectra are contaminated by additive components at both low and high frequencies. High frequency contamination often results from instrumental noise (arising in the voltage clamp input stage), which increases with f due to the presence of a membrane capacitance. This contamination is dependent on the membrane impedance. Therefore, although additive, it cannot be removed by the background subtraction method outlined below. The high frequency contamination may be amended by lowering f_3 so that contaminated data points are not included in the integrations. More difficult cases are dealt with by analyzing the tissue impedance and the amplifier noise characteristics.

Low frequency contamination often arises from back-

[1] If the data $y(f)$ distribute randomly around the theoretical curve $Y(f)$ and the record is of sufficient length, then $\int_{f_1}^{f_2}[y(f) - Y(f)]\,df = 0$, or $\int_{f_1}^{f_2} y(f)\,df = \int_{f_1}^{f_2} Y(f)\,df$.

[2] Christensen and Bindslev (1982) took advantage of integration in order to analyze Lorentzians, although they still used recursive fitting.

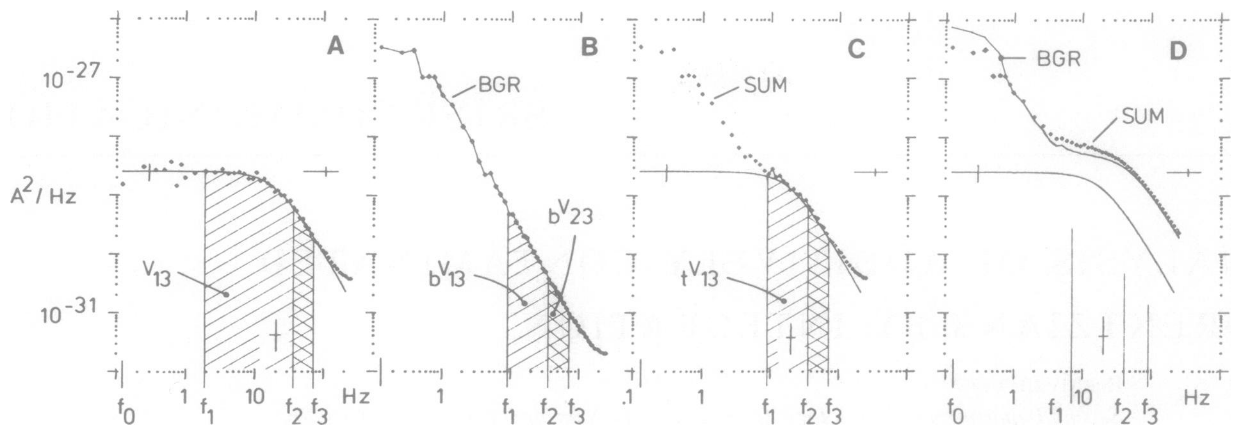

FIGURE 1 Current power density spectra (one-sided) based on pseudo–first-order switching kinetics. The integration limits used for analysis, f_1, f_2, and f_3, are indicated. The hatched areas would represent bandwidth-limited variances if the plots were in linear coordinates. (*A*) Lorentzian data generated with the rate constants, $k_{on} = 100/s$ and $k_{off} = 10/s$. At $f > f_3$, the data points deviate from the expected Lorentzian values because of aliasing. The smooth curve was found by using Eqs. 4 and 2a. The standard deviation of the estimate, indicated at G_O on the left, is that of the lowest-frequency points. These points were excluded from the analysis by choosing $f_1 > f_0$. The standard deviation on the right is that of the data point (at f_1) that was determined least accurately among those that were used. The standard deviation of data points from the Lorentzian, in the frequency band f_0–f_c, was found to be 8% larger than the standard deviation that is indicated on the left. Hamilton's R-factor (Hamilton, 1964. p. 158) was estimated to be 0.445 for the frequency band f_0–f_3. f_c and its standard deviation is indicated at 20 Hz. (*B*) Background spectrum (BGR) generated as a Lorentzian tail using $k_{on} = k_{off} = 1/s$, $f_c < 1$ Hz. The indicated f_1, f_2, and f_3 are identical to those of panel *C*. (*C*) Composite spectrum (SUM) obtained by adding the power densities of panel *A* and *B*. f_1, f_2, and f_3 were selected interactively from a display of these data. Eqs. 4–6 and 2a were used for analysis, yielding the smooth Lorentzian shown. It is nearly identical to the Lorentzian of panel *A* and did not change appreciably when f_1 was lowered to f_0. By subtracting BGR from SUM, Lorentzian data points may be obtained and plotted around the smooth Lorentzian found. The empirical power-sample variance, the confidence limits of G_O and f_c, and the relative misfit (Hamilton's R-factor) may then be calculated by standard procedures. Furthermore, the hypothesis that states that the difference of the two spectra is a Lorentzian may be checked with the chi-square test or the run test (Bendat and Piersol, 1971; p 122). If these tests fail, the additivity requirement may be violated. (*D*) The total spectrum (points labeled SUM) was generated as the sum of the Lorentzian spectrum from panel *A* and a background spectrum (which is itself the sum of two Lorentzians). When SUM had been obtained, the background spectrum was altered by adding power at low frequencies. The spectrum labeled BGR was thus obtained and used as the background spectrum in the analysis. The deviation of BGR from SUM at low frequencies might have resulted from unequal drifting in background and total data records. Note that the BGR slope becomes less negative at intermediate frequencies. Analysis retrieved the Lorentzian (shown as a smooth curve), which is identical to that of panel *A* and *C*. Clearly, the method is insensitive to violations of the additivity requirement at $f < f_1$.

ground noise sources that are in parallel with the source of Lorentzian noise. In such cases, the spectra of the two sources are additive and a subtraction procedure may be used to separate the Lorentzian noise from the background noise. Particularly in work with epithelia, the method of multiparameter-nonlinear least-squares regression analysis is often used to determine at once G_O, f_c, and two parameters of the background spectrum. It is assumed that the background spectrum has a certain shape, which is verified occasionally by blocking the Lorentzian process completely (e.g., Van Driessche and Zeiske, 1980; Zeiske et al., 1982; Li and Lindemann, 1983; Henrich and Lindemann, 1983; Loo et al., 1983). To obtain good results, weight factors may be used to decrease the influence of low-frequency data (Conti et al., 1976).

To improve the accuracy and decrease the number of parameters that have to be determined, it is recommended that one also record the background fluctuations (while the Lorentzian process is blocked), preferably after each recording of the total fluctuations. This is particularly feasible when, as in most of the papers just cited, extrinsic channel blockers like amiloride are used that block channel conductance completely at high concentrations. In these cases, complete blockage is used anyway to estimate the mean background current, which is subtracted from the total current in order to calculate the mean current I_L through the channels with Lorentzian switching kinetics. In the many cases where this subtraction is valid, the following treatment is also valid.

By numerical integration we calculated the bandwidth-limited variances $_bV_{13}$ and $_bV_{23}$ from the background spectrum as well as $_tV_{13}$ and $_tV_{23}$ from the composite, or total, spectrum. The Lorentzian variances were then found from the equations:

$$V_{13} = {}_tV_{13} - {}_bV_{13}, \quad (5)$$

$$V_{23} = {}_tV_{23} - {}_bV_{23}. \quad (6)$$

(An equivalent procedure would be to subtract the background spectrum from the total spectrum and integrate the resulting difference spectrum.) Next, Eq. 4 and Eq. 2a were used to calculate f_c and G_O of the Lorentzian. Note that no assumptions about the shape of the background spectrum entered the analysis. The sole requirement for the use of the procedure is that Lorentzian fluctuations and background fluctuations are additive in the frequency range f_1–f_3.

To demonstrate the procedure, stochastic open/close patterns of a single channel were generated for given rate constants by means of a Monte Carlo procedure, which uses a shot current of 10^{-13} A and a sample rate of 500 Hz. Records representing 82 s of sample time were thus accumulated and divided into 10 blocks of 4,096 samples. A time-window function and anti-aliasing were not used. The blocks of one record were Fourier-transformed and the power spectra (one-sided) were linearly condensed, averaged, and displayed in double-logarithmic coordinates. Given the rate constants of blockage, the following values were expected from records of infinite length: $I_L = 0.91 \cdot 10^{-14}$ A, $V_{04} = 0.786 \cdot 10^{-27}$ A^2, $G_O = 0.3 \cdot 10^{-28}$ A^2/Hz, and $f_c = 17.51$ Hz. The values found for Fig. 1 *A* were $I_L = 0.764 \cdot 10^{-14}$ A, $V_{04} = 0.744 \cdot 10^{-27}$ A^2, $G_O = 0.252 \cdot 10^{-28} \pm 0.036 \cdot 10^{-28}$ A^2/Hz, and $f_c = 20.5 \pm 2.9$ Hz. Deviations from the expected values were mainly a result of the limited record length. [The standard deviation specified for G_O is the standard deviation of a "spectral estimate" (of a data point), as defined by Bendat and Piersol (1971, p. 329). Following Anderson and Stevens (1973), the values given were based on the averaging and condensing of data points that was done at the lowest frequency that entered the analysis, i.e., at f_1. The standard deviation for f_c was estimated approximately, using the relative error of G_O.] In Fig. 1 *A*, f_1 was purposely chosen to be rather high in order to show that when low-frequency data points are excluded, the result does not deteriorate. By choosing $f_1 = f_0$, the values found for G_O and f_c changed negligibly.

The background spectrum of Fig. 1 *B* was generated in the same way, but with smaller rate constants. The data points of Fig. 1 *C* were obtained by adding the two spectra. These points were analyzed together with the integrals of the background spectrum, yielding the Lorentzian shown (smooth curve in Fig. 1 *C* with $G_O = 0.253 \cdot 10^{-28}$ A^2/Hz and $f_c = 20.4$ Hz). The Lorentzian that was found is indistinguishable from that of Fig. 1 *A*. Note that f_1 was chosen to be rather high, which barred low-frequency points from entering the analysis. Thereby, low-frequency drifting, which may differ in background and total spectral data, can be eliminated.

The integration method is particularly useful in those cases where the background spectrum alters its slope at intermediate or high frequencies. A rather extreme example that deals with this kind of background spectrum is provided in Fig. 1 *D*, which shows that retrieval of G_O and f_c is perfect. Furthermore, the method is insensitive to violations of the additivity requirement at $f < f_1$.

The choice of f_1 (within the limits $f_0 \leq f_1 \leq 0.5 \cdot f_c$) depends on the validity of the additivity requirement at low frequencies. In bad cases, a trial and error procedure starting at $f_1 = f_0$ will find the best possible result (see legend of Fig. 1 *C*). However, the task of picking spectral limits (f_1, f_3) for the analysis may also arise in recursive fitting. Unique for the integration method is merely that a third limit, f_2, has to be chosen. I recommend that following procedure to remove arbitrariness from this choice: After picking f_1 and f_3, the integration is first done with $f_2 = 10^{0.5(\log f_1 + \log f_3)}$. Thus a good approximation of f_c is usually obtained and f_2 is set to this value. Then the integration is repeated. In consequence all final results are obtained uniformly with $f_2 \simeq f_c$.

If the process to be analyzed is represented by a double Lorentzian that results, for instance, from the action of two competitive blockers (e.g., Lindemann and Van Driessche, 1978), then four integrals of appropriately spaced limits will be required. The four Lorentzian papameters are obtained by solving four simultaneous nonlinear equations. The conventional alternative would be to use recursive nonlinear regression analysis with at least six free parameters.

The programs written for this study (FORTRAN IV) are available on request.

The research was supported by the Deutsche Forschungsgemeinschaft through SFB 38, project C1.

Received for publication 21 October 1983 and in final form 2 May 1984.

REFERENCES

Anderson, C. R., and C. F. Stevens. 1973. Voltage clamp analysis of acetylcholine produced end-plate current fluctuations at frog neuromuscular junction. *J. Physiol. (Lond.)*. 235:655–691.

Bendat, J. S., and A. G. Piersol. 1971. Random Data: Analysis and Measurement Procedures. Wiley-Interscience, New York. 407.

Christensen, O., and N. Bindslev. 1982. Fluctuation analysis of short-circuit current in a warm-blooded sodium-retaining epithelium: site current, density, and interaction with triamterene. *J. Membr. Biol.* 65:19–30.

Conti, F., B. Hille, B. Neumcke, W. Nonner, and R. Stämpfli. 1976. Measurement of the conductance of the sodium channel from current fluctuations at the node of Ranvier. *J. Physiol. (Lond.)*. 262:699–727.

Hamilton, W. C. 1964. Statistics in Physical Science. Ronald Press, New York. 230.

Henrich, M., and B. Lindemann. 1983. Voltage dependence of channel currents and channel densities in the apical membrane of toad urinary bladder. *In* Intestinal Absorption and Secretion. E. Skadhauge and K. Heintze, editors. MTP Press Ltd., Lancaster, PA. 209–220.

Li, J. H. -Y., and B. Lindemann. 1983. Competitive blocking of epithelial Na-channels by organic cations: the relationship between macroscopic and microscopic inhibition constants. *J. Membr. Biol.* 76:235–251.

Lindemann, B., and W. Van Driessche. 1978. The mechanism of Na uptake through Na-selective channels in the epithelium of frog skin. *In* Membrane Transport Processes. J. F. Hoffman, editor. Raven Press, New York. 155–178.

Loo, D. D. F., S. A. Lewis, M. S. Ifshin, and J. M. Diamond. 1983. Turnover, membrane insertion, and degradation of sodium channels in rabbit urinary bladder. *Science (Wash. DC)*. 221:1288–1290.

Van Driessche, W., and W. Zeiske. 1980. Na^{2+}-induced conductance fluctuations of spontaneously fluctuating K^+ channels in the apical membrane of frog skin (*Rana temporaria*). *J. Membr. Biol.* 56:31–42.

Zeiske, W., N. K. Wills, and W. Van Driessche. 1982. Na^+ channels and amiloride-induced noise in the mammalian colon epithelium. *Biochim. Biophys. Acta*. 688:201–210.